Mechanical Properties of (Fe-Cr)-Reinforced C-Al-Si-Ti Coatings Prepared by Flame Spray Technique

Maha A. Shaker*, Ali I. Salih

Department of Physics, College of Science, University of Kirkuk, Kirkuk, IRAQ
* Corresponding author email: scpm24004@uokirkuk.edu.iq

Abstract
In this work, flame spray technique was used to deposit coatings of C-Al-Si-Ti reinforced with different contents of Fe-Cr alloy on stainless steel surfaces to protect these surfaces from corrosion due to their continuous exposure to mechanical stresses and high temperatures. Spray parameters were controlled to develop much more homogeneous and dense microstructures. An optimal ratio of the reinforcing material was determined to achieve highest values of hardness and coating adhesion, making these coatings good candidates for engineering applications operating in harsh environments that require high resistance to corrosion and mechanical stresses.

Keywords: Flame spray; Physical properties; Cermet coatings; Fe-Cr alloy
Received: April 2026; **Revised:** May 2026; **Accepted:** May 2026; **Published:** July 2026

1. Introduction

Among the various thermal spraying techniques flame spraying is widely used in industrial applications due to its relatively low operational cost and simplicity of equipment [1–4]. However, coatings produced by this method commonly suffer from two major limitations weak adhesion to the substrate and high internal porosity which negatively affect the required mechanical and thermal performance [5–8]. To overcome these limitations, the use of interfacial (bond) layers has been introduced as an effective approach to enhance coating performance by improving adhesion strength, reducing thermal residual stresses, and enhancing overall coating integrity [9–12]. This study investigates the effect of introducing a (Fe–Cr) interlayer on a (C–Al–Si–Ti) based coating system to evaluate its influence on the mechanical and physical properties of flame-sprayed coatings and to correlate these properties with microstructural evolution The (C–Al–Si–Ti) coating system used in this study consists of a (metal–ceramic) composite mixture based on carbon , aluminum , silicon , and titanium powders with specified weight ratios and particle size ranges as presented in (Table 1) in the experimental Part (Fe–Cr) alloys were selected as bonding materials due to their intermediate thermal expansion coefficient , The selection of Fe–Cr as an interlayer is further supported by its intermediate coefficient of thermal expansion which is typically in the range of 11-13 $\times 10^{-6}$ K^{-1}. This value lies between that of stainless steel substrates (approximately 16-17 $\times 10^{-6}$ K^{-1} and ceramic-rich C-Al-Si-Ti coatings (approximately 6-10 $\times 10^{-6}$ K^{-1}) . This graded thermal expansion behavior helps to reduce thermal mismatch between the coating and substrate thereby minimizing residual thermal stresses generated during cooling and improving interfacial adhesion and coating stability [11]. which lies between metallic substrates and ceramic coatings making them suitable candidates for reducing thermal mismatch and improving interfacial stability [13-15] . The Fe–Cr interlayer composition used in this work contained 18.26 wt.% Cr with the balance Fe . Despite extensive research on thermally sprayed coatings, most previous studies have focused primarily on single-layer systems while limited attention has been given to dual-layer configurations incorporating interfacial bonding layers [16-18]. Therefore, the present study aims to evaluate the effect of introducing an Fe–Cr interfacial layer on the mechanical properties of flame-sprayed C-Al-Si-Ti coatings deposited on stainless steel substrates The investigated properties include hardness, adhesion strength, and surface roughness.

2. Experimental Part

Stainless steel (304L) substrates were coated with C-Al-Si-Ti metal-ceramic composite coatings reinforced with Fe-Cr at different volumetric contents as listed in table (1). The coatings were deposited using a Rototec 80 flame thermal spraying system operated with oxygen and acetylene gases at pressures of 0.7 and 0.4 bar, respectively. A spraying

distance of 15-20 cm and a spray angle of 90° were maintained during deposition, while the particle velocity reached approximately 100 m/s. The composite base material (C-Al-Si-Ti) exhibited good resistance to elevated temperatures as the melting temperatures of its constituent components exceeded 1200°C depending on their compositional ratios making the material suitable for flame thermal spraying applications Prior to coating, the stainless steel substrates were thoroughly cleaned with alcohol to remove grease and contaminants followed by mechanical surface roughening to enhance coating adhesion to the substrate. The samples were then thermally annealed in an electric furnace at temperatures ranging from 850 to 1050 °C for 90 min to stabilize the coating structure. The selection of this temperature range is based on its ability to promote interfacial diffusion, stress relaxation, and microstructural stabilization in thermally sprayed coatings. At lower temperatures, sufficient atomic mobility is activated to improve inter-particle bonding whereas the upper temperature limit was selected to avoid excessive grain growth and possible phase instability. Therefore, this range represents an optimized thermal window commonly used for improving the structural integrity and mechanical performance of thermal spray coatings [3,21,22]. In the present study, the same heat treatment range (850-1050°C) was applied to all samples. The obtained mechanical properties (hardness and adhesion strength) exhibited a consistent overall trend across all heat-treated samples indicating that the effect of thermal exposure was generally uniform within the investigated range. Therefore, the results are discussed in terms of the overall influence of heat treatment rather than separating the contribution of each individual temperature. The mechanical and surface properties of the coatings, including hardness, adhesion strength, and surface roughness, were evaluated. The obtained results were interpreted according to well-established thermal spray mechanisms reported in the literature, while detailed phase and microstructural analyses are recommended for future work to further support interfacial evolution and coating behavior [3]. Figure (1) shows the St. St. 304L specimen used as a substrate in order to ensure experimental reproducibility and to provide a clear description of the prepared test specimens.

The mechanical properties of the prepared samples mainly hardness and adhesion strength, were determined. Five readings were taken for all samples from different sides to ensure the consistency and repeatability of the results Adhesion strength was evaluated using a Universal Testing Machine according to the ASTM C633 standard via the pull-off test method [3]. The obtained adhesion values were found to be within the acceptable range commonly reported for thermally sprayed coating systems taking into account the influence of coating composition, substrate condition, and processing parameters on interfacial bonding behavior. Two types of specimens were examined unreinforced coatings and Fe-Cr reinforced coatings to determine the interfacial bonding strength between the coating and the substrate. Surface roughness was measured using a profilometer where three readings were taken for each sample and the average value was recorded to ensure accuracy [5]. Surface roughness and adhesion measurements were conducted on separately tested samples prepared under identical processing conditions.

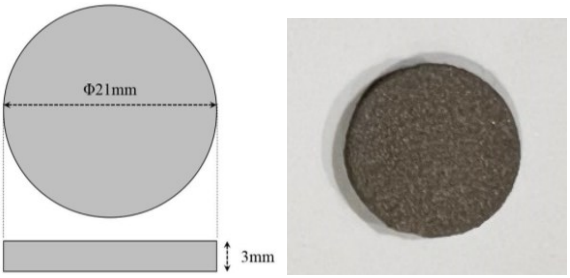

Fig. (1) Top and front view and dimensions of the St. St. 304L substrate (left), and a photograph of the coated sample (right)

3. Results and Discussion

Figure (2) shows the effect of the chromium content in the Fe-Cr alloy on Vickers hardness after heat treatment. Hardness gradually increases with increasing chromium content due to the formation of a solid solution that inhibits dislocation movement, reaching a maximum value of 177 kg/mm^2 at approximately 8%. After this percentage hardness begins to decrease as a result of changes in the microstructure and the formation of less effective strengthening phases or carbides .This behavior may also be associated with local microstructural inhomogeneity and particle agglomeration at higher reinforcement contents.

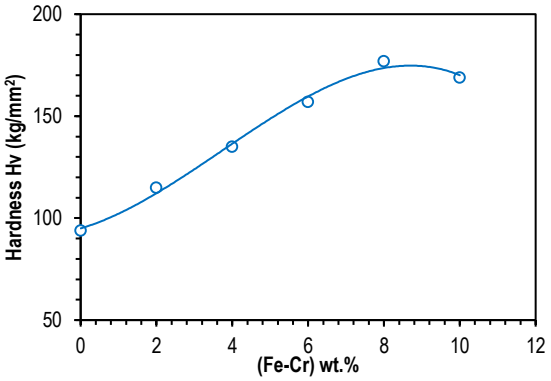

Fig. (4) Effect of reinforcing material content on the Vickers hardness after heat treatment

Although carbide precipitates can improve hardness by restricting dislocation movement

excessive precipitation may reduce matrix ductility and negatively affect the balance between hardness and toughness. Since detailed phase characterization was not performed in the present study these interpretations are based on commonly reported mechanisms in thermally sprayed composite coatings [20-22]. This is consistent with what was mentioned in a previous study on the effect of microstructure and phase distribution in determining hardness values [19]. Therefore, there is an optimal chromium content that achieves the highest hardness, and any increase beyond it leads to a deterioration of mechanical properties.

Figure (5) illustrates a non-linear relationship between the Fe–Cr alloy content and the adhesion strength after heat treatment. The adhesion strength starts at its lowest value for the unreinforced sample (21 MPa) then increases significantly with increasing Fe-Cr content, reaching a maximum value of 37 MPa at 8 wt.% Fe-Cr. Beyond this point, the curve shows a minor decrease up to 10 wt.%. The increase in adhesion strength is attributed to improved interfacial bonding and enhanced mechanical interlocking between the coating and substrate, as supported by thermal spray literature [22]. However, although surface roughness continues to increase up to 10 wt.% the adhesion strength does not follow the same trend, indicating that adhesion is governed not only by roughness but also by the effective interfacial contact quality At higher Fe-Cr contents (8-10 wt.%) excessive surface irregularities and coating heterogeneity promote interfacial void formation and stress concentration, which reduce bonding efficiency. The 8 wt.% addition represents an optimum condition where maximum coating–substrate cohesion is achieved This behavior demonstrates the dominance of interfacial integrity over surface roughness at high reinforcement levels.

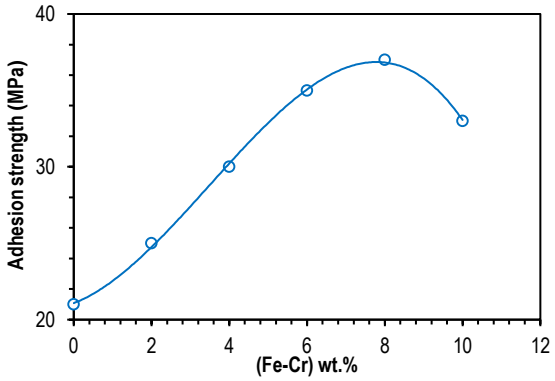

Fig. (5) Effect of reinforcement addition on adhesion strength after heat treatment

Figure (6) illustrates the relationship between Fe-Cr alloy content and surface roughness after heat treatment. Excessive roughness may reduce the effective contact area and introduce interfacial discontinuities that negatively affect coating adhesion. In addition, variations in particle flattening behavior coating densification and porosity evolution with increasing reinforcement content contribute to the development of a more heterogeneous surface. The increase in roughness within the range of 9.5-11.9 µm indicates a transition in surface morphology; however, beyond an optimum level, the beneficial effect of mechanical interlocking may be counterbalanced by increased defect density and localized stress concentration sites at the interface. Therefore, the simultaneous increase in surface roughness and its influence on adhesion behavior can be attributed to the competing effects of mechanical anchoring and interfacial integrity degradation in agreement with previously reported findings in thermal spray coating systems [21].

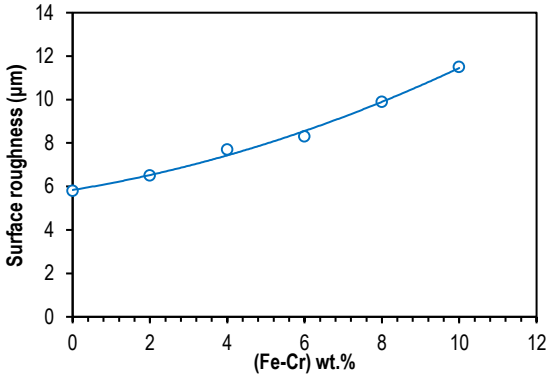

Fig (6) Effect of reinforcement addition on surface roughness after heat treatment

4. Conclusions

This study demonstrates a clear improvement in mechanical properties of flame-sprayed C-Al-Si-Ti coatings with Fe-Cr reinforcement particularly in hardness and adhesion strength. Compared with the unreinforced coating the optimized composition (8 wt.% Fe-Cr) shows a significant increase in hardness from 90 to 180 kg/mm² (≈100% improvement) and in adhesion strength from 20 to 35 MPa (≈75% improvement). These results indicate that the selection of an appropriate reinforcing ratio is a key factor in optimizing coating performance by enhancing load-bearing capacity and interfacial bonding.

References

[1] S.Y. Darweesh, R.A. Rasheed and M.A. Abdullah, "Treatment of failures in turbine blades by cermet coatings", *J. Failure Anal. Prevent.*, 23(6) (2023) 2461-2470.

[2] S. Ariharan et al. (eds.), **"Fundamentals of Thermal Spraying"**, CRC Press (2022).

[3] L. Pawlowski, **"The science and engineering of thermal spray coatings"**, John Wiley & Sons (2008).

[4] R.K. Bishwas, M.A. Alam and S.A. Jahan, "Crystallographic and morphological characterization of high-crystalline α-alumina nanoparticles: A comprehensive X-ray diffraction and transmission electron microscopy study", *Chem. Phys. Lett.*, 878 (2025) 142245.
[5] S. Batool et al., "Metal-free heteroatom integrated defect engineering of flexible carbon networks on tin oxide nanoparticles to enhance lithium-ion battery performance", *Adv. Compos. Hybrid Mater.*, 8(1) (2025) 6.
[6] M. Fellah et al., "Thermal treatment effect on structural and mechanical properties of Cr–C coatings", *Trans. IMF*, 96(2) (2018) 79-85.
[7] S. Saini et al., "Tunability of characteristics of novel PMMA/ZnO/SnO_2 (PZS) polymer nanocomposites", *Mater. Res. Innov.*, 29(7) (2025) 483-498.
[8] J.A. Venables, G.D.T. Spiller and M. Hanbucken, "Nucleation and growth of thin films", *Rep. Prog. Phys.*, 47(4) (1984) 399-459.
[9] M.I. Boulos, P.L. Fauchais and J.V. Heberlein, **"Thermal Spray Fundamentals: From Powder to Part"**, Springer (NY, 2021).
[10] S.M. Ghareeb, S.M. Aman Allah and S.Y. Darweesh, "Compressive strength, wear, and structure characteristics as a result of silicon carbide addition on a copper base", *J. Phys.: Conf. Ser.*, 1999(1) (2021) 012040.
[11] W.D. Callister Jr. and D.G. Rethwisch, **"Materials Science and Engineering: An Introduction"**, John Wiley & Sons (2020).
[12] S.J. Galpin, "A review of microstructure phenomena during manufacture of polycrystalline Ni-based superalloys", *Mater. Sci. Technol.*, 38(16) (2022) 1315-1331.
[13] K.A. Khor et al., "Microstructure and mechanical properties of plasma sprayed HA/YSZ/Ti–6Al–4V composite coatings", *Biomaterials*, 25(18) (2004) 4009-4017.
[14] S. Naib et al., "Crack driving force prediction in heterogeneous welds using Vickers hardness maps and hardness transfer functions", *Eng. Fracture Mech.*, 201 (2018) 322-335.
[15] E.J. Salih, S.M.A Allah and S.Y. Darweesh, "Study the structural and mechanical properties of the Cu-WC composite", *AIP Conf. Proc.*, 2398(1) (2022) 020035.
[16] M. Caro et al., "Lattice thermal conductivity of multi-component alloys", *J. Alloys Compd.*, 648 (2015) 408-413.
[17] J. Mascenik and T. Krenicky, "Advanced Production, Processing and Characterization of Industrial Materials", *Materials*, 18(23) (2025) 5366.
[18] G.Y. Koga et al., "An overview of thermally sprayed Fe-Cr-Nb-B metallic glass coatings: from the alloy development to the coating's performance against corrosion and wear", *J. Therm. Spray Technol.*, 31(4) (2022) 923-955.
[19] M.K. Hassan, "Recent development on fragmentation, aggregation and percolation", *J. Phys. A: Math. Theor.*, 55(19) (2022) 191001.
[20] L. Łatka et al., "Review of functionally graded thermal sprayed coatings", *Appl. Sci.*, 10(15) (2020) 5153.
[21] S. Kumar and R. Kumar, "Influence of processing conditions on the properties of thermal sprayed coating: a review", *Surf. Eng.*, 37(11) (2021) 1339-1372.
[22] J.R. Davis (ed.), **"Handbook of thermal spray technology"**, ASM international (2004).

Table (1) Composition of the used materials

Powder	Purity (%)	Particle Size	Morphology	Supplier
C	47.14 %	75-100 μm	Flake-like	Castolin+Eutectic
Al	33.17 %	75-100 μm	Irregular/Spherical	Castolin+Eutectic
Si	8.78 %	75-100 μm	Angular	Castolin+Eutectic
Ti	8.05 %	75-100 μm	Spherical	Castolin+Eutectic
Fe-Cr alloy	79.65% Fe, 18.62% Cr	45-75 μm	Irregular	Castolin+Eutectic

